RSC Advances

RSC Advances

www.rsc.org/advances

ROYAL SOCIETY OF CHEMISTRY

www.rsc.org/advances

Journal Name

ARTICLE TYPE

RSC Advances Accepted Manuscript

Intracellular pH-sensitive Delivery CaCO₃ Nanoparticles Templated by Hydrophobic Modified Starch Micelles

Xiaoying Ying [a], Chunlei Shan [a], Kuaikuai Jiang [a], Zhong Chen [a,*], Yongzhong Du[a,*]

A novel method of preparing CaCO₃ nanoparticles using a starch-octanoic acid micelle as the template was engineered. The CaCO₃ nanoparticles engineered via this method displayed stable physiochemical properties, high drug-
10 **encapsulation efficiency, low cell cytotoxicity and an intracellular pH-sensitive release profile, which indicate the potential for further application.**

Targeted drug delivery systems (TDDSs) are advanced drug delivery systems through which drugs accumulate into a targeted
15 tissue, organ, cell or intracellular organelle after administration. TDDS has numerous advantages for drug delivery, including a higher drug concentration in the targeted site, longer action time, and reduced toxicity and drug dose.

However, TDDS is not yet commonly used in the clinic,
20 mainly because of the limitations of target distribution and insufficient drug release at the targeted site. To solve these problems, various drug carriers with environmentally sensitive properties were explored [1]. pH sensitive drug carriers may be the most widely used variety. The physiological basis for pH
25 sensitive targeted delivery is that tumor sites are more acidic than normal tissues [2, 3], and intracellular organelles such as endosomes and lysosomes also have a low pH value (~4.5) [2]. Various nanosized pH sensitive carriers have been developed, including dendrimers [4, 5], liposomes [6, 7], micelles [8-11], and polymeric
30 nanoparticles [12]. These carriers display excellent pH sensitivity, yet their use in physiological conditions is limited because of their organic composition. In this respect, inorganic materials are superior [13] and easy to synthesize [14].

Calcium carbonate (CaCO₃) is a common endogenic inorganic
35 compound with good solubility in acid, which make it a potential pH sensitive drug carrier. Drug-loaded CaCO₃ nanoparticles are stable in neutral and weakly basic environments, meaning that there would be minimal or no drug release in systemic circulation. When the nanoparticles reach the tumor site or enter tumor cells,
40 which are both weak acidic environments, the CaCO₃ nanoparticles become degraded, releasing the drug [15]. CaCO₃ nanoparticles have a high specific surface area, are easy to synthesize and modify, have low bio-toxicity, are not environmentally toxic [16, 17] and have been used in TDDS [18-22]. A
45 number of templates are used to regulate the preparation of CaCO₃ nanoparticles, such as starch[15], polyelectrolyte [23, 24], stearic acid monolayer [25], and protein[26].

In this study, a starch-octanoic acid chemical conjugate (ST-OA) was synthesized as a novel template to improve drug loading
50 and the pH-sensitive drug release of CaCO3 nanoparticles (**Scheme 1**). Starch-octanoic acid was synthesized via an ester linkage between the hydroxyl group of a glucose monomer and the carboxyl group of octanoic acid.
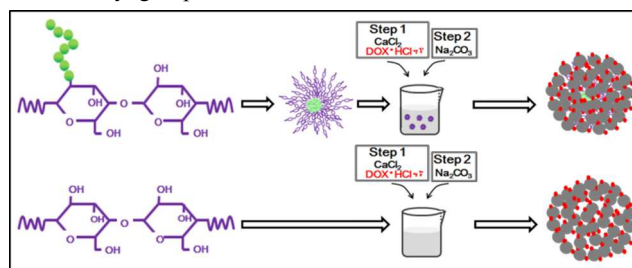
Scheme 1. The preparation schemes of CaCO₃ nanoparticles using starch
55 and starch-octanoic acid templates.
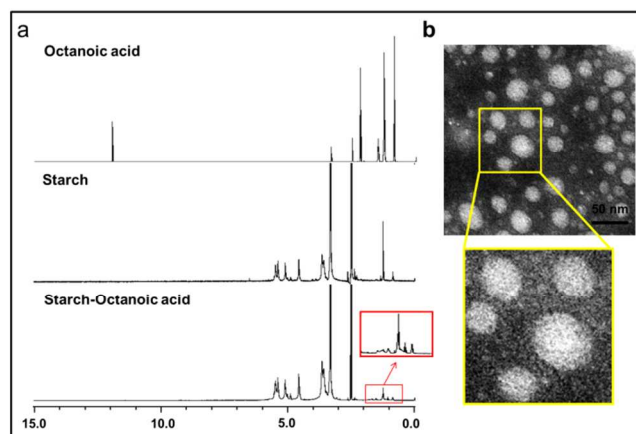
Figure 1. (a) ¹H-NMR spectra of octanoic acid, starch and starch-octanoic acid; (b) TEM images of starch-octanoic micelles.

Fig. 1a shows the ¹H-NMR spectra of octanoic acid, starch and
60 synthesized starch-octanoic acid. The characteristic peak of the carboxyl (-COOH) in octanoic acid appeared at 11.964 ppm, the peak of methylene adjacent to carboxyl appeared at 2.184 ppm, and the methyl (-CH₃) and methylene (-CH₂) in octanoic acid ranged from approximately 1.2-1.5 ppm. The characteristic
65 hydroxyl (-OH) peak of starch appeared at 1.2 ppm, and the hydrogen on the pyranoid ring appeared between 3.6-5.5 ppm

(3.7, 4.6, 5.1, 5.4, 5.5 ppm). In the spectrum of the synthesized product, the peak of hydrogen on the pyranoid ring and the peaks of methyl ($-CH_3$) and methylene ($-CH_2$) in octanoic acid (1.5-2.0 ppm) remained (the red box). The characteristic peak of the carboxyl disappeared, while the peak signal strength of the hydroxyl (-OH) on starch decreased (the red box), indicating that the carboxyl had been replaced and the starch was partly grafted to octanoic acid.

Starch-octanoic acid is composed of hydrophilic starch and hydrophobic octanoic acid and forms micelles at the critical micelle concentration (CMC) by self-assembly. The CMC value was determined to be 40.6 μg•mL^{-1} (Fig. S1). The morphology of the micelles was observed using a transmission electron microscope (TEM). The ST-OA micelles exhibited a spherical shape, and their sizes were distributed narrowly between 30-40 nm (Fig. 1b).

CaCO₃ nanoparticles were prepared using a 0.25% starch solution and ST-OA micelle dispersions at various concentrations (0.25%, 0.125% and 0.0625%) labeled as Blank-A, Blank-B, Blank-C, Blank-D, respectively. The nanoparticles were evaluated using infrared spectrum analysis (Fig. S2), and their physicochemical properties were also determined. The size measurement results are shown in Table 1. The size distribution of the four blank nanoparticles was similar, approximately 420 nm. The morphologies of the blank nanoparticles were also observed using scanning electron microscopy (SEM) (Fig. S3) and TEM (Fig. 2 a-d). The images indicated that the sizes were well distributed between 400-500 nm and the nanoparticles were sphere shaped.

Table 1. Physicochemical properties of prepared blank and DOX-loaded CaCO3 nanoparticles.

	Size (nm)	PI	EE (%)
Blank-A	413±47.4	0.088	--
Blank-B	423±43.8	0.113	--
Blank-C	410±48.5	0.064	--
Blank-D	412±49.5	0.124	--
DOX loaded-A	576±67.5	0.039	8.38±0.34
DOX loaded-B	483±67.5	0.155	13.05±0.52
DOX loaded-C	548±48.0	0.132	16.46±1.03
DOX loaded-D	579±85.8	0.183	19.83±0.74

Doxorubicin is a widely researched anticancer drug [26, 27]. Doxorubicin (DOX)-loaded nanoparticles were prepared and labeled as DOX loaded-A, DOX loaded-B, DOX loaded-C, and DOX loaded-D.The drug encapsulation efficiencies of the DOX-loaded nanoparticles are shown in Table 1. The EE% of the DOX-loaded nanoparticles formed in starch solution was 8.375%, which was significantly lower than that of the nanoparticles formed in starch-octanoic acid micelle templates. The EE% of DOX-loaded B, C, and D nanoparticles were 13.05%, 16.46% and 19.83%, approximately 1.6-, 2- and 3-folds of DOX-loaded-A nanoparticles, respectively. The morphology of the DOX-loaded nanoparticles was observed with a scanning electron microscope (SEM). As shown in Figure 2 (e-h), the nanoparticles exhibited a spherical shape, and their sizes were distributed at approximately 500 nm, which are similar to the results found by Zetasizer (Table 1). Moreover, as shown by the SEM images (Fig. 2, f, g and h), the B, C and D nanoparticles had rough surfaces, which were formed from smaller CaCO₃ nanoparticles. The increased drug encapsulation efficiency of the CaCO₃ nanoparticles templated by ST-OA micelle dispersion was due to

their morphology, which had a larger specific surface area.

After loading, the sizes of the DOX-loaded A, B, C, and D nanoparticles were 576 nm, 483 nm, 543 nm and 579 nm, respectively (Tab. 1), which were larger than the blank nanoparticles. The increased size might originate from the drug loading. Notice that the size of the DOX-loaded nanoparticles templated by the ST-OA micelle dispersion increased with drug loading. At the end of the drug loading, the size of the DOX-loaded nanoparticles templated by the ST-OA micelle dispersion was smaller than that of those templated by starch, which might indicate a higher stability of the CaCO₃ nanoparticles prepared
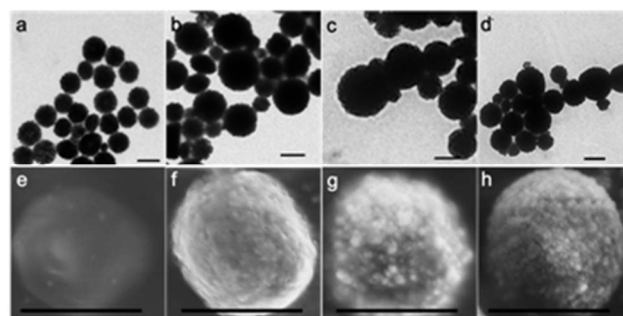
using the ST-OA micelle dispersion.

Figure 2. TEM and SEM images of the blank and DOX-loaded CaCO₃ nanoparticles synthesized using a 0.25% starch solution (a, e) or 0.25%, 0.125%, and 0.0625% starch-octanoic acid micelle dispersions (b and f; c and g; d and h). The bars represent 0.5 μm.

Figure 3a shows the release of DOX from the DOX-loaded nanoparticles at pH 7.4. The nanoparticles formed in starch exhibited a faster release, but less DOX was released overall. The cumulative drug-release percentage of the DOX-loaded-A nanoparticles was less than 25% after 72 h, indicating that minimal DOX would be released from the nanoparticles in general circulation. The performance of the nanoparticles formed in starch-octanoic acid micelle dispersions was extremely similar. Before 12 h, almost equivalent amounts of DOX were released, while nearly no DOX was released after 12 h. This effect may be caused by the quick release of the DOX adhered to the surface of nanoparticles, while the
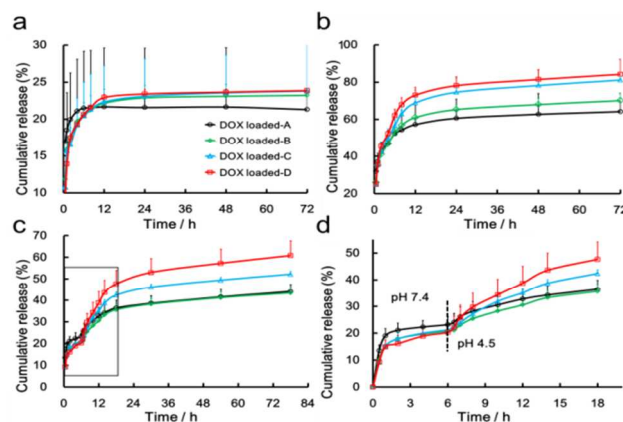
Figure 3. In vitro drug release profiles of DOX-loaded nanoparticles in different pH medium: (a) In pH 7.4 PBS for 72 h; (b) In pH 4.5 PBS for 72 h; (c) In pH 7.4 PBS for the first 6 h and in pH 4.5 PBS for 72 h thereafter; (d) In pH 7.4 PBS for the first 6 h and in pH 4.5 PBS for 12 h

thereafter (this figure was enlarged from figure (c)). (n=3)

loaded DOX does not release in these conditions. In pH 4.5 medium, the DOX released from the nanoparticles clearly increased in first 12 h and gradually plateaued thereafter.
5 Approximately 65% of the DOX loaded into the A nanoparticles was released, less than that of the B, C, and D nanoparticles (70%, 81%, and 84%, respectively) after 72 h. To simulate the in vivo transport of the $CaCO_3$ nanoparticles, a drug release assay was conducted at pH 7.4 for the first 6 h and at pH 4.5 for the next 72
10 h. For the first 6 h, the release of DOX from the different nanoparticles was similar at pH 7.4. However, after 6 h, the DOX-loaded-C and D nanoparticles released more DOX. At 72 h, approximately 50% and 60% DOX was released from C and D nanoparticles, respectively. The final drug release in the dual pH
15 mediums experiment was lower than in the pH 4.5 medium only experiment, possibly because in the pH 7.4 medium the Ca^{2+} and PO_4^{3-} formed $Ca_3(PO_4)_2$, which was less soluble. $Ca_3(PO_4)_2$ may adhere to the surface of the nanoparticles and obstruct drug release. These results prove these four $CaCO_3$ nanoparticles can
20 be used for targeted drug delivery based on different pH environments and that the $CaCO_3$ nanoparticles formed in the 0.125% and 0.0625% starch-octanoic acid template dispersions are most feasible.

An intracellular uptake assay in A549 cells was then
25 conducted. After incubation with DOX•HCl or DOX-loaded nanoparticles for 1 or 3 h, the cells were washed and observed using an inverted fluorescence microscope (Fig. 4a). The cellular uptake of the Dox-loaded nanoparticles was time dependent, and the Dox-loaded-B nanoparticles had a faster cellular uptake
30 ability, possibly because the DOX-loaded-B nanoparticles had the smallest size. It has been proven that a small particle size contributes to endocytosis.
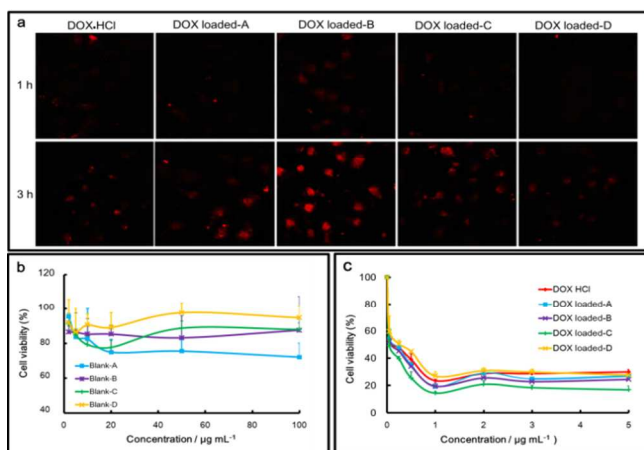
Figure 4. (a) The fluorescence after A549 cells were incubated with DOX-loaded nanoparticles for 1 or 3 h; (b) and (c) cell viabilities after
35 A549 cells were incubated with blank $CaCO_3$ nanoparticles (b) or DOX-loaded $CaCO_3$ nanoparticles (c) for 48 h. The untreated cells were used as a positive control. The experiments were repeated three times (n=3).

Figures 4b and 4c show the cytotoxicities of blank and DOX-
40 loaded $CaCO_3$ nanoparticles, respectively. The cell viabilities after incubation with blank nanoparticles for 48 h at the tested concentration were above 70%, showing that $CaCO_3$ nanoparticles had no obvious cytotoxicity and were appropriate

for use as drug carriers. The DOX-loaded-C nanoparticles
45 showed more cell toxicity than DOX•HCl, and their IC_{50} was 0.0391μg•ml^{-1}. The IC_{50} of DOX•HCl and the DOX-loaded-A, B, and D nanoparticles were 0.0723, 0.0769, 0.0584 and 1.713 μg•mL^{-1}, respectively. The low IC_{50} of the DOX-loaded-C nanoparticles may be because of the higher cellular uptake and
50 faster drug release at the lower pH. Although the DOX-loaded-D nanoparticles had the fastest drug release at the lower pH, its cellular uptake was too slow. The results indicate that DOX-loaded nanoparticles are effective inhibitors of tumor cell growth, especially the DOX-loaded-C nanoparticles. Compared to
55 DOX•HCl, the DOX-loaded-A and B nanoparticles performed slightly better, while the DOX-loaded-D nanoparticles did not.

Conclusions

The $CaCO_3$ nanoparticles prepared using a starch-octanoic acid micelle dispersion as the template had higher DOX
60 encapsulation efficiencies, faster tumor cellular uptake and a rougher surface to achieve faster drug release under acidic conditions. These properties allow for in vivo antitumor targeted drug delivery.

Notes and references

^{a} *College of Pharmaceutical Sciences, Zhejiang University, 866*
70 *Yuhangtang Road, Hangzhou 310058 (P. R. China)*
Fax: 0571-88208439;
Tel: 0571-88208439;
E-mail: duyongzhong@zju.edu.cn, chenzhong@zju.edu.cn

75 1 S. Ganta, H. Devalapally, A. Shahiwala, M. Amiji, *J.Control. Release.* 2008, **126**, 187.
2 L.E. Gerweck, K. Seetharaman, *Cancer. Res*. 1996, **56**, 1194.
3 J.L. Wike-Hooley, J. Haveman, H.S. Reinhold, Radiother. *Oncol*. 1984, **2**, 343.
80 4 Y.G. Jin, X. Ren, W. Wang, L.J. Ke, E.J. Ning, L.N. Du, J.Bradshaw. *Int. J. Pharma*. 2011, **420**, 378
5 H. Yuan, K. Luo, Y.S. Lai, Y.J Pu, B. He, G. Wang, Y. W, Z.W. Gu, *Mol. Pharmaceutics*. 2010, **7**, 9.
6 E.Yuba, N. Tajima, Y. Yoshizaki, A. Harada, H. Hayashi, K. Kono,
85 *Biomaterials*.2014, In press.
7 E. Ducat, J. Deprez, O. Peulen, B. Evrard, G. Piel, *Drug Dis. Today.* 2010, **15**, 1083.
8 G.H. Gao, Y.Li, D.S. Lee, *J.Control. Release.* 2013, **169**, 180.
9 Y.H. Liu, W.P. Wang, J.H. Yang, C.M. Zhou, J. Sun, *Asian J. Pham.Sci.*
90 2013, **8**, 159
10 Y.Q. Yang, B. Zhao, Z.D. Li, W.J. Lin, C.Y. Zhang, X.D. Guo, J.F. Wang, L.J. Zhang, *Acta Biomat*. 2013, **9**, 7679
11 J. Liu，H.X. Li, X.Q. Jiang, C. Zhang，Q.N. Ping, *Carbo.Poly*. 2010, **82**, 432.
95 12 M. Shen, Y.Z. Huang, L.M Han, J. Qin, X.L Fang, J.X. Wang, V. C. Yang, *J. Control. Release*. 2012, **161**, 884.
13 M. Arruebo, *Nanobiotechnol*. 2012, **4**, 16.
14 C.Y. Peng, Q.H. Zhao, C.Y. Gao, *Collo ids Surf. A*. 2010, **353**, 132.
15 W. Wei, G.H. Ma, G. Hu, D. Yu, T. Mcleish, Z.G. Su, Z.Y. Shen, *J.*
100 *Am. Chem. Soc*. 2008, **130**, 158.
16 S. Haruta, T. Hanafusa, H. Fukase, H. Miyajima, T. Oki, Diabetes Technol. *Ther*. 2003, **5**, 1.
17 S. Huang, J.C. Chen, C.W. Hsu, W.H. Chang, *Nanotechnology*. 2009, **20**, 375102.

18 X.M. Ma, L.P. Li, L. Yang, C.Y. Su, Y.M. Guo, K. Jiang, *Mat.Let.* 2011, **65**, 3176.

19 Y. Ueno, H. Futagawa, Y. Takagi, A. Ueno, Y. Mizushima, *J. Controlled.Release*.2005, **103**, 9.

20 S. Haruta, T.Hanafusa, H.Fukase, H.Miyajima, T.Oki, *Diabetes Technol. Ther.*2003, **5**, 1.

21 Y. Svenskay, B. Parakhonskiy, A. Haased, V. Atkin, E. Lukyanetse, D. Gorin, R. Antolinid, *Bio.Chem.* 2013, **182**, 11.

22 S.K.Kim, M.B. Foote, L. Huang, *Cancer Let.* 2013, **334**,311.

23 J.G. Yu, H. Guo, S. A. Davis, *Adv. Funct. Mater.* 2006, **16**, 2035.

24 H. Tang, J. Yu, X. Zhao, *J. Alloy. Compd.* 2008, **463**, 343.

25 E.M. Pouget, P.H.H. Bomans, J.A.C.M. Goos, P.M. Frederik, G. de With, N.A.J.M. Sommerdijk. *Science*. 2009, **323**, 1455.

26 X.M. Ma, H.Y. Yang, H.F. Chen, L. Yang, Y.M. Guo, Y.Y. Si, *J. Cryst. Growth*. 2011, **327**, 146.

27 Y.Z. Du, L.L. Cai, P. Liu, J. You, H. Yuan, F.Q. Hu, *Biomaterials*.2012, **33**, 8858.

28 Y.Z. Du, Q. Weng, H. Yuan, F.Q. Hu, *ACS nano*.2010, **4**, 6894.